Transfer of germanium to marine sediments: insights from its accumulation in radiolarites and authigenic capture under reducing conditions. Some examples through geological ages.

Nicolas Tribovillard, Viviane Bout-Roumazeilles, Armelle Riboulleau, François Baudin, Taniel Danelian, Laurent Riquier

Transfer of germanium to marine sediments: Insights from its accumulation in radiolarites and authigenic capture under reducing conditions. Some examples through geological ages

N. Tribovillard[a,*], V. Bout-Roumazeilles[a], A. Riboulleau[a], F. Baudin[b], T. Danelian[a], Laurent Riquier[c]

[a] Université Lille 1, Géosystèmes Lab, FRE CNRS 3298, bâtiment SN5, 59655 Villeneuve d'Ascq cedex, France

[b] Université Pierre et Marie Curie-Paris 6, Institut des Sciences de la Terre de Paris, UMR CNRS 7193, 75252 PARIS cedex 05, France

[c] Université de Bourgogne, Biogéosciences Lab, UMR CNRS 5561, 21000 Dijon, France

[*] Corresponding author. E-mail address: Nicolas.Tribovillard@univ-lille1.fr (N. Tribovillard).

Keywords: Germanium - Ge/Si – Radiolarites - Redox conditions - Sedimentary geochemistry

Abstract

In the geosphere, germanium (Ge) has a chemical behavior close to that of silicon (Si), and Ge commonly substitutes for Si (in small proportions) in silicates. Studying the evolution of the respective proportions of Ge and Si through time allows us to better constrain the global Si cycle. The marine inventory of Ge present as dissolved germanic acid is facing two main sinks known through the study of present sediments: 1) incorporation into diatom frustules and transfer to sediments by these "shuttles", 2) capture of Ge released to pore water through frustule dissolution by authigenic mineral phases forming within reducing sediments. Our goals are to determine whether such a bio-induced transfer of Ge is also achieved by radiolarian and whether Ge could be

trapped directly from seawater into authigenic phases with no intervention of opal-secreting organisms (shuttles). To this end, we studied two Paleozoic radiolarite formations and geological formations dated of Devonian, Jurassic and Cretaceous, deposited under more or less drastic redox conditions. Our results show that the Ge/Si values observed for these radiolarites are close to (slightly above) those measured from modern diatoms and sponges. In addition, our results confirm what is observed with some present-day reducing sediments: the ancient sediments that underwent reducing depositional conditions are authigenically enriched in Ge. Furthermore, it is probable that at least a part of the authigenic Ge came directly from seawater. The recurrence and extent (through time and space) of anoxic conditions affecting sea bottoms have been quite important through the geological times; consequently, the capture of Ge by reducing sediments must have impacted Ge distribution and in turn, the evolution of the seawater Ge/Si ratio.

1. Introduction

Germanium (Ge) and silicon (Si) have similar chemical properties in the marine environment (e.g., Froelich and Andreae, 1981; Froelich et al., 1985a,b; McManus et al., 2003): in addition to their similar ionic and covalent radii, typical coordination for Si and inorganic Ge is tetrahedral and both dissolved species (silicic and germanic acids) can be present in seawater as tetravalent hydroxide complexes (e.g., Bernstein, 1985; Pokrovski and Schott, 1998). Consequently, the marine cycles of inorganic Ge and Si are tightly coupled and substitution of Ge for Si in mineral phases in seawater is common (e.g., Kolodny and Halicz, 1988; Bernstein, 1985; Pokrovski and Schott, 1998). The two main sources of Ge and Si to the ocean are mineral weathering and hydrothermal fluids (see more detailed information in Table 1 and references therein). The main sink for Si and Ge removal from the ocean is the transfer to sediments via incorporation into biogenic opal (main opal-secreting organisms

are diatoms, radiolarians and sponges) followed by burial, but Ge has an additional sink, namely, loss via non-opal phases during sediment early diagenesis. The differences in the relative importance of the source terms for Ge and Si, combined with the fact that siliceous microfossils may record the Ge/Si ratio of the water column, has led to the proposal that the Ge/Si ratio recorded in diatoms could serve to monitor the relative importance of these two sources through time (e.g., Froelich and Andreae, 1981; Froelich et al., 1985a, Froelich et al., 1985b, Mortlock and Froelich, 1987; Froelich et al., 1989; Shemesh et al., 1989; Mortlock et al., 1993). Pioneer works in the 70's suggested that there was no discrimination between Si and Ge during frustule construction relative to the seawater Ge/Si ratio (Azam et al., 1973; Azam, 1974; Azam and Chisholm, 1976). However recent works have demonstrated the possibility for a faint biologic fractionation but its impact is not significant (e.g., Bareille et al., 1998; Ellwood and Maher, 2003; Ellwood et al., 2006; Sutton et al., 2010).

Following modeling showing that more Ge is supplied to the seas than can be removed by diatom frustule accumulation in the sediments (see details about the "Ge missing sink" in, e.g., Chester, 2000), a number of papers (based on pore water profile data, benthic incubation data, whole-core incubation data or water column data) now suggest that Ge can be removed from the ocean to marine sediments partly independently of Si (Murnane et al., 1989; Hammond et al., 2000; King et al., 2000; McManus et al., 2003). McManus et al. (2003) shows that iron-rich continental margin sediments sequesters Ge, which balances the global Ge budget. King et al. (2000) indicates that authigenically fixed Ge may be associated with authigenic U, or authigenic Fe phase such as bacterially mediated magnetite or an authigenic Fe-rich clay mineral. The authigenic capture of Ge would preferably take place in reducing, organic matter rich sediments (King et al., 2000; Hammond et al., 2000; McManus et al., 2003). The papers referred to above consider that Ge is dominantly transferred from seawater to sediment via diatom frustules and that Ge, released to pore

water through opal dissolution, may be subsequently trapped into Fe- (or U-) rich authigenic phases. It may be questioned: 1) whether radiolarians can also be efficient Ge shuttles from seawater to sediments, and 2) whether Ge can be trapped by sediment directly from the bottom seawater reservoir (with no role played by opal shuttles) under reducing depositional conditions, favoring U- and possibly Mo-authigenic enrichment of sediments.

The present paper aims to bring some elements of response to these questions. To compare the respective roles of radiolarians and diatoms in the transfer of Ge to the sediments we studied two radiolarite formations, and to examine the potential authigenic capture of Ge by reducing sediments, we studied here various Devonian, Jurassic or Cretaceous sedimentary rocks deposited under more or less severely reducing conditions: Kimmeridgian–Tithonian geological formations of the Boulonnais area (northern France), the Tunisian Bahloul Formation recording the Cenomanian–Turonian boundary, Cretaceous deposits of the Weddell Sea (ODP leg 113, site 692B), late Devonian rocks of the La Serre Section (southern France) that recorded the Frasnian–Famennian boundary. Germanium data are very rarely reported in the literature devoted to sediments and sedimentary rocks. This scarcity is explained by the small number of studies considering Ge in sedimentary settings and by the fact that the chemical analyses of sediments that use HF-digestion preclude Si and Ge concentration measurement (Si- and Ge-fluorides are evaporated – and lost – during HF digestion). To our knowledge, this paper presents the first report on a rather large data set about Ge concentrations in radiolarites and, above all, in ancient sediments deposited under reducing (oxygen-restricted) bottom conditions.

2. Sources of particulate Ge to the sediments and study of radiolarites

The sediments collect Ge from two main origins: 1) the detrital fraction comes with the terrigenous particles; 2) the biogenic fraction comes from the

seawater: silica-secreting organisms (diatoms, radiolarians and sponges) incorporate Ge into their hard parts and act as a Ge shuttle when their frustules, skeletons or spicules settle to the sea bottom.

Due to its propensity to substitute for Si, Ge is present in most silicates, usually in low concentrations (up to a few fig μg^{-1} or ppm). Germanium concentrations within silicate minerals depend on the specific silicate group. Germanium concentration decreases in the following order: nesosilicates (e.g., topaz, garnet and olivine), sorosilicates (e.g., epidote and zoisite), inosilicates (e.g., amphibole and pyroxenes), phyllosilicates (e.g., muscovite, biotite and chlorite) and tectosilicate (e.g., quartz, plagioclase and K-feldspar); consequently, Ge is generally observed to be enriched in olivine and pyroxene relative to quartz and feldspar but the variation of the Ge content with the geological environment is of greater significance (see review by Höll et al., 2007 and references therein). A compilation of various databases (e.g., Wedepohl, 1971, 1991; Taylor and McLennan, 1985; McLennan, 2001) indicate that the abundance of Ge in the upper continental crust ranges between 1.3 and 1.6 ppm and that the most currently used value for land-derived particulate supply is 1.6 ppm. Consequently, the weight ratio of Ge to Si in the clastic fraction of marine sediments is estimated to be 5.19·10−6 (according to McLennan, 2001). The corresponding molar ratio is 2.01 μmol mol^{-1}.

Germanium dissolved in seawater originates from continental weathering and submarine hydrothermalism (details and references in Höll et al., 2007). The reactive part of the marine Ge inventory is under the form of germanic acid $Ge(OH)_4$ or H_4GeO_4 that shows a nutrient-like distribution in oceans. Germanium is also present as methylated forms that are stable to degradation and display a conservative profile in seawater (e.g., Bruland and Lohan, 2003). The marine organisms secrete their opal hard parts using the dissolved silicic acid of seawater where the molar ratio of Ge to Si is Ge/Si=0.72 μmol Ge per mol Si (or $1.86 \cdot 10^{-6}$ in weight proportions). Diatoms are reported to incorporate

Ge to their opal frustule with a Ge/Si ratio ranging from 0.45 to 0.78 μmol/mol (Froelich et al., 1989, 1992; Hammond et al., 2000; King et al., 2000; McManus et al., 2003; Ellwood and Maher, 2003). The weight ratio is consequently in the range: $1.16 \cdot 10^{-6}$–$2.02 \cdot 10^{-6}$. Sponges are reported to incorporate Ge to their opal spicule with a Ge/Si ratio of only 0.075– 0.380 μmol/mol (Ellwood et al., 2006), or $0.20 \cdot 10^{-6}$–$0.98 \cdot 10^{-6}$ (weight ratio). To our knowledge, no such Ge/Si data for radiolarians are available in the literature. To try and fill partly this gap, we took into consideration two radiolarite sample sets.

3. Materials and methods

3.1. Studied formations

3.1.1. Radiolarites

We studied 13 samples of the late Cambrian-middle Ordovician Burubaital Formation of Kazakhstan and 6 samples of the late Devonian-early to middle Permian Chiang Dao Chert Formation of Thailand. Just in a few words, the Burubaital Formation is made of chert deposits that form several nappes composing a tectonic mélange within a subduction–accretion complexe. The complexe was formed along the active margin of an Arenigan–Llandeilian volcanic island arc (details in Tolmacheva et al., 2001). The radiolarian cherts are mainly red but locally vary to black and green. Single chert beds are usually 3– 10 cm thick, occasionally 20 cm thick, with poorly defined layers of brownish-red (1–5 cm thick) siliceous shale intercalated (Tolmacheva et al., 2001). The radiolarites of the Burubaital Formation recorded deep-sea (abyssal) biogenic sedimentation. They accumulated at equatorial/subequatorial paleolatitudes in an area of upwelling (Tolmacheva et al., 2001).

The Chiang Dao Chert Formation is characterized by a huge radiolarite body (200 m thick) made of chert beds (3 to 10 cm thick) with thin, intercalated shale levels (Randon et al., 2006). The samples studied here are dated of Frasnian–Visean; they were deposited in deep oceanic environments (details in

Randon et al., 2006 and references therein).

3.1.2. Formations deposited under more or less reducing conditions

We study here various geological formations that are already well described in the literature. Consequently, only a very brief description will be given below, along with some key references where extensive description can be found. We only give here the minimum description required for the purpose of this paper. Most of these sediments (carbonates, marls and shales) were deposited under suboxic to anoxic or even strongly euxinic conditions, based on independent paleoredox criteria described in each supporting paper. Formally, the depositional conditions are generally classified according to the concentration in dissolved O_2 and H_2S as oxic (>2.0 ml O_2 L^{-1}), dysoxic or suboxic (~0.2–2.0 ml O_2 L^{-1}), anoxic–non sulfidic (<0.2 ml O_2 L^{-1}, 0.0 ml H_2S L^{-1}), and anoxic–sulfidic or euxinic (0.0 ml O_2 L^{-1}, >0 ml H_2S L^{-1}) (Savrda and Bottjer, 1991; Wignall, 1994). Practically, concerning ancient sediments for which O_2 and H_2S concentrations cannot be measured, the classification is basing on the paleoposition of the so-called redox-cline, i.e., the frontier separating conditions with free oxygen dissolved in porewaters (aerobic conditions) from conditions with no dissolved oxygen (anaerobic conditions). Oxic sediments correspond to conditions where the redox-cline was lying at some depth below the sediment–water interface; suboxic sediments correspond to conditions where the redox-cline was at shallow depth below the sediment–water interface. Anoxic conditions are when the redox-cline corresponds to the sediment–water interface and euxinic conditions are when the redox-cline hangs over the sediment–water interface and when sulfate-reducing reactions can produce within the water column, hence releasing free H_2S into the seawater. For a detailed presentation and discussion of this redox classification, see Tyson (1995) and Canfield and Thamdrup (2009).

3.1.2.1. The Frasnian–Famennian boundary (late Devonian) at the LaSerre Section (France).

The famous Frasnian–Famennian boundary was a major period of biodiversity loss and environmental changes, and was also the time of significant climatic variations. The Upper Frasnian interval is generally associated with the deposition of one or two organic-rich units in outer shelf and epicontinental basin settings, i.e. the so-called Kellwasser (KW) horizons. These beds have been recognized in many sections, located on the borders of Laurasian (N. America and N. Europe), Gondwanan (S. Europe and Africa), South China and on the southern border of the Siberian continents. Numerous factors controlling the KW organic-rich sediment accumulation have been proposed, such as increased primary productivity or bottom-water oxygen-depleted conditions. These factors have been connected to different driving mechanisms acting in isolation or combined, such as sea-level fluctuations, climatic variations, land plants spreading, volcanism or mountain building (Averbuch et al., 2005; Riquier et al., 2006, 2007, and references therein). In France, the Frasnian–Famennian boundary section is best exposed in several trenches on the southern slope of the La Serre hill (Montagne Noire; Feist, 1985). The interval of the section considered starts with light grey calcilutites rich in pyrite and benthic biota. They are abruptly overlain by a sequence of alternating dark brownish and black, fissile marls and platy thin-bedded bituminous marly limestones. The levels at the base of this alternation are considered to be equivalent to the Upper Kellwasser horizon. The La Serre equivalent may constitute a rather distal and basinal variant of the typical Kellwasser limestone that was deposited on submarine rises (Tribovillard et al., 2004a and references therein).

3.1.2.2. The Jurassic formations of the Boulonnais area (northern France).

The deposits of the famous Kimmeridge Clay Formation accumulated

during the late Jurassic in the distal part of an epicontinental sea extending from the Barents Sea to the English Channel. The Kimmeridge Clay Formation has been extensively studied, notably owing to the large oil-source rock potential of coeval rocks in the North Sea grabens. In the present paper, we study the proximal lateral equivalent deposits, cropping alongshore, north of Boulogne-sur-mer. These sediments accumulated on a mix siliciclastic- carbonate ramp subject to dominantly aerobic conditions with some episodes of dissolved oxygen restriction (Proust et al., 1995; Deconinck et al., 1996).

The Kimmeridgian Argiles de Châtillon Formation is made up with dark marls, mudstones and shales with high marine-origin organic matter content. The hemi-pelagic paleoenvironments have been determined as oxic to anoxic through both geochemical and paleontological lines of evidence. The rocks contain a mixture of terrestrial and marine organic matter but the marine-origin organic matter is exclusively sulfurized in the samples containing TOC>6–7% (Tribovillard et al., 2001, 2002, 2004b).

The Tithonian Bancs Jumeaux Formation consists of dark marls, mudstones and siltstones with moderate marine-organic matter content deposited on a mix carbonate-siliciclastic ramp. The paleoenvironments have been determined as suboxic. The rocks contain a mixture of terrestrial and marine organic matter (Tribovillard et al., 2008).

The Tithonian Argiles de Wimereux Formation consists of dark marls, mudstones and siltstones with moderate to low organic-matter content, deposited on a mix carbonate-siliciclastic ramp. The paleoenvironments have been determined as normally oxygenated to suboxic. The rocks contain a mixture of dominant terrestrial and accessory marine organic matter.

3.1.2.2.1. The Weddell Sea (ODP leg 113).

ODP Hole 692B (70°43.432"S, 13°49.195"W) was drilled in the eastern Weddell Sea on the shelf of the Dronning Maud Land. The site is located on the

flank of a submarine canyon, the so-called Wegener Canyon, by 2875 m of water (Barker et al., 1988). Early Cretaceous black shales were penetrated between Cores 113-692B-7R and 113-692B-12R. The 22.2 m of recovered sediments, described as Unit III (Barker et al., 1988), consist of black to very dark grey claystone and mudstone, with varying percentages of clay, carbonate, and organic matter. Parallel lamination is the dominant sedimentary structure; bioturbation is occasionally observed. The sediments are interpreted to have accumulated in an outer shelf/upper slope environment.

The Bahloul Formation of Tunisia was deposited during the wellknown oceanic anoxic event OAE2 occurring around the Cenomanian– Turonian boundary (Caron et al., 1999 and references therein). This formation can be followed from the margin of the Saharian platform (southern Tunisia) to the deep Tethyan Basin to the North, yielding important thickness variations. The Bahloul Formation was deposited in a marine basin strongly influenced by thermohaline-type circulation depending mainly on climatic fluctuations. The studied section crops out in the Wadi Bahloul riverbed in Central Tunisia (Caron et al., 1999 and references therein). The formation shows regular alternations of black laminated limestone beds and bioturbated grey marls. The black laminated facies were deposited under suboxic/anoxic conditions whereas the grey marls were deposited under more frequently oxygenated conditions.

3.2. Geochemical analysis and enrichment factor calculation

For all the samples referred to in this study, the chemical analyses either already published or not) were performed by ICP-AES (major and minor elements) and ICP-MS (trace elements) at the spectrochemical laboratory of the Centre de Recherches en Pétrographie et Géochimie of Vandoeuvre-les-Nancy (French Centre National de la Recherche Scientifique). The samples were prepared by fusion with $LiBO_2$, followed by HNO_3 dissolution. Precision and accuracy were both better than 1% (mean 0.5%) for major-minor elements and

8% for trace metals, as checked by international standards and analysis of replicate samples (Table 2; Carignan et al., 2001).

In some occasions, the enrichment factors were calculated for some trace metals as follows: X-EF=[$(X/Al)_{sample}$ / $(X/Al)_{crustal}$], where X and Al represent the weight % concentrations of element X and Al, respectively. Samples were normalized using the upper-crust compositions of McLennan (2001), i.e., Al: 8.04%, Ge: 1.6 ppm or μg g−1. The calculation uses Al normalization. The Al normalization is commonly used to minimize dilution effects by carbonate and biogenic silica, for example, but the approach can be problematic as evoked below (for a discussion, see Van der Weijden, 2002, and Tribovillard et al., 2006). The virtue of using enrichment factors is that any value larger than 1 points to enrichment relative to crustal abundance.

We refer herein below to the contents or enrichments of the sediments or rocks in U and Mo, because both elements are wellknown and frequently-used redox proxies (extensive reviews in Algeo and Maynard, 2004; Brumsack, 2006; Tribovillard et al., 2006). A recent paper (Algeo and Tribovillard, 2009) illustrated how the enrichments in each of the two elements may be simultaneously used to decipher paleoredox conditions of depositional environments suspected to have been concerned with (benthic) oxygen restriction.

4. Results

4.1. Ge/Si ratio from radiolarites

4.1.1. Burubaital Formation

The 13 samples show SiO_2 and Al_2O_3 contents ranging between 95.0% and 99.1% (mean 97.1%), and between 0.1% and 2.3% (mean 0.8%), respectively, with a Ge content bracketed between 0.32 ppm and 1.76 ppm (mean 0.79 ppm; Table 3). The two samples with the lowest Al_2O_3 content have a Ge/Si weight ratio of $2.31 \cdot 10^{-6}$ and $3.85 \cdot 10^{-6}$, respectively. The corresponding

molar ratios are 0.89 and 1.49 µmol mol−1, respectively.

4.1.2. Chiang Dao Chert Formation

The 6 samples show SiO_2 and Al_2O_3 contents ranging between 85.6% and 98.3% (mean 91.2%), and between 0.6% and 7.7% (mean 3.0%), respectively, with a Ge content bracketed between 1.48 ppm and 3.10 ppm (mean 1.81%; Table 3). The two samples with the lowest Al_2O_3 content (0.62% and 0.78%) have a Ge/Si weight ratio of $3.30 \cdot 10^{-6}$ and $3.40 \cdot 10^{-6}$, respectively (corresponding molar ratios 1.28 and 1.31 µmol mol−1, respectively).

The two radiolarite formations show the presence of aluminum, that is, of a detrital fraction made of aluminosilicates. The detrital fraction is higher in the Chiang Dao Chert than in the Burubaital Formation. The former formation shows a positive linear correlation (R^2=0.945; n=6) between Al_2O_3 and Ge/Si, whereas such a correlation does not exist for the Burubaital Formation (R^2=0.166; n=13). These observations indicate that some correction is needed to have a better estimate of the Ge/Si ratio of pristine radiolarites, i.e., with no "pollution" by the detrital fraction of the rock. Basing upon average crustal composition, one can make an estimate of how much Ge is present from detrital material (Table 3). The terrigenous part of the Ge content (Ge_{terr}) is calculated as following:

$Ge_{terr} = Al_{sample} \times (Ge/Al)_{crustal}$. The biogenic Ge ($Ge_{bio}$) is then obtained as: $Ge_{bio}=Ge-Ge_{terr}$. The biogenic fraction of the Si content is calculated in the same way. Thus, following this procedure, one can estimate the value of the Ge/Si ratio corresponding to the biogenic fractions of the rock [$(Ge/Si)_{bio}$]. Table 3 shows that the $(Ge/Si)_{bio}$ weight ratio is bracketed between $0.56 \cdot 10^{-6}$ and $3.85 \cdot 10^{-6}$ (average $1.61 \cdot 10^{-6}$ or 0.62 µmol mol−1) for the Burubaital Formation and between $3.24 \cdot 10^{-6}$ and $9.71 \cdot 10^{-6}$ (average $4.06 \cdot 10^{-6}$ or 1.57 µmol mol−1) for the Chiang Dao Chert. The latter formation thus keeps showing higher values than the former, in spite of the correction that removed

the detrital fractions of Ge and Si from the total Ge and Si content.

4.2. Authigenic enrichment in reducing sediments

4.2.1. La Serre Section — Frasnian–Famennian boundary (Devonian)

The La Serre Section is made up with carbonate rocks ($CaCO_3$=52.6%–96.8%, mean 88.1%). Consequently, the Al_2O_3 content is very low (0.30%–6.51%, mean 1.41%) and this is one case where AL normalization of trace-metal contents is not recommended (Van der Weijden, 2002; Tribovillard et al., 2006). Thus, enrichment factors are not calculated and non-normalized concentrations in trace elements are considered. Due to very high carbonate contents, low trace-metal concentrations are expected, which is the case for Ge but not for U, with U ranging between 3 and 13 ppm (Fig. 1).

A Al_2O_3 vs. SiO_2 diagram (Fig. 1A) shows a good correlation between both parameters, thus indicating most SiO_2 comes dominantly with the aluminosilicate fraction and not from quartz grains or opal hard parts. SiO_2 is poorly correlated to the Ge content (Fig. 1B). Most of the samples have Ge concentrations below or close to 0.2 ppm; two samples stand out with higher Ge concentrations, these two samples are also those with the highest U contents (Fig. 1C). The same is true concerning Mo. Both samples come from the upper Kellwasser Horizon.

4.2.2. The Jurassic of the Boulonnais

4.2.2.1. The Argiles de Wimereux Formation.

A Al_2O_3 vs. SiO_2 diagram shows a positive tendency linking both parameters, with two samples shifting toward high SiO_2 and low Al_2O_3 (Fig. 2A). These two samples also shift out of the clear correlation drawn between SiO_2 and Ge contents (Fig. 2B), showing a relative depletion in Ge. All the samples yield enrichment-factor (EF) values ranging between 1 and 2 for U and 0.4 and 1.2 for Mo (Fig. 2C), which means that no enrichment is detected for

both redox proxies. The EF values for Ge are ranging between 1.0 and 1.6 for all samples but two with EF close to 2.1 and 2.2, respectively.

4.2.2.2. The Argiles de Châtillon Formation.

The situation is quite similar in this case (Fig. 2D to F), where the samples showing enrichment in SiO_2 relative to Al_2O_3 (Fig. 2D) also show a relative depletion in Ge compared to SiO_2 (Fig. 2E). Here again, U and Mo do not show any significant enrichment: EF values are in the 1.0–3.5 range for Mo and 1.1–1.6 for U. Lastly, Ge shows EF values ranging between 1.0 and 1.2.

4.2.2.3. The Bancs Jumeaux Formation.

The situation is somewhat different in the case of the Bancs Jumeaux. The Al_2O_3 vs. SiO_2 relationship shows some scatter (Fig. 2G) but a clear correlation is drawn between SiO_2 and Ge concentrations. Two points with high Ge content shift somewhat out of the sample distribution, indicating a relative enrichment in Ge compared to the SiO_2 content (Fig. 2H). Within the 17 sample data set, eight samples shows Ge-EF close to or below the value 1.0, eight samples are ranging between 1.4 and 2.0, and one sample reaches the value 2.6 (Fig. 2I). The three samples with the highest Ge-EF have also the highest Mo-EF values (15–50) but only the sample with Ge-EFN2.5 shows the highest U-EF (close to 100).

4.2.3. The Weddell Sea site — Early Cretaceous

A Al_2O_3 vs. SiO_2 diagram shows a clear positive correlation between the two parameters (Fig. 3A). Fig. 3B shows that the Ge and SiO_2-contents are rather correlated but show some scatter. A U-EF vs. Mo-EF crossplot shows a concomitant enrichment in U and Mo about in the same proportion (Fig. 3C) and Fig. 3D shows a positive trend linking U-EF to Ge-EF. If only samples with U-EFN5 are considered (i.e., samples for which a U-EF is detected; Algeo and Tribovillard, 2009), a correlation is drawn between U-EF and Ge-EF with a

correlation coefficient of 0.979 (determination coefficient R^2=0.958).

4.2.4. The Bahloul Formation — Upper Cretaceous

The samples of the Bahloul Formation draw a nice correlation between Al_2O_3 and SiO_2 (Fig. 4A, R^2=0.926, n=12). The correlation is rather good between SiO_2- and Ge-contents, but the determination coefficient is somewhat lower (R^2=0.828). A U-EF vs. Mo-EF crossplot shows a good correlation (Fig. 4C). Fig. 4D illustrates the samples with a detectable (close to or above EF=5) or significant (EFN10) enrichment factor for Mo are those with high values for Ge-EF.

5. Interpretation

5.1. Ge/Si of radiolarites

The depositional setting of the two radiolarites was far from any source of coarse detrital particles but the sea bottom most probably received small, possibly air borne particles such as clay minerals. The Al-corrected SiO_2 content of the samples may be considered as approximately representing the opal supply by radiolarians and the Al-corrected Ge content must represent the fraction that is trapped in the opal skeletons and transferred to the sediment. Silica mobilization most probably occurred (perhaps even massively) during radiolarite diagenesis; however little is known about a possible Si-Ge "fractionation" during solution migration and we cannot take this point into consideration. In addition, we do not know whether radiolarians incorporate Ge into their opal at equilibrium with the seawater Ge/Si ratio. Largely, diatom frustules are considered to represent the seawater Ge/Si ratio (Shemesh et al., 1988, 1989) but the same is not necessarily true for radiolarian skeletons and this point requires further study. Finally, we have no or little idea of the evolution of the Ge/Si ratio of seawater throughout geological times. The germanium budget of the Paleozoic oceans might have been different from the

present situation. Consequently, with all these limitations, we are able to produce here only a rough estimate of the Ge/Si of radiolarian opal. This estimate suggests (Ge/Si)bio values (weight proportions) averaging 1.61·10−6 (or 0.62 μmol mol−1) for the Burubaital Formation, and averaging 4.06·10−6 (or 1.57 μmol - mol−1) for the Chiang Dao Chert. The lower (Ge/Si)bio of the Burubaital Formation suggests the contribution of silica with a comparatively lower Ge/Si ratio: for instance the presence of sponge spicules or the influence of silica from interstitial water poor in Ge during diagenesis.

Thus, it is observed in the present work that the values of the Ge/Si weight ratio are of the same order of magnitude either for the detrital supply (~$5.19\cdot10^{-6}$ or 2.01 μmol mol−1) or for the biogenic ones: $1.61\cdot10^{-6}$–$4.06\cdot10^{-6}$ for radiolarians (0.62–1.57 μmol mol−1), $0.20\cdot10^{-6}$–$0.98\cdot10^{-6}$ for sponges (0.08–0.38 μmol mol−1), $1.16\cdot10^{-6}$–$2.02\cdot10^{-6}$ for diatoms (0.45–0.78 μmol mol−1; Fig. 1). These numbers also suggest that the detrital input transfers more abundant Ge to sediment than biogenic opal does, but the ratio values must be taken with caution. In other words, these observations mean that the contrasting nature of Ge-bearing particles, either clastic or biogenic, will not impact drastically the value of the Ge/Si ratio in sediments or sedimentary rocks but, according to the data reported here, the Ge/Si ratio of detrital particles is always higher than that of biogenic particles (Fig. 5). Conversely, it is inferred that sediments enriched in Ge relative to Si either lost proportionally more Si than Ge during burial and diagenesis or accumulated Ge through an authigenic process capturing more Ge than Si. The former hypothesis suggests a marked post-depositional decoupling of Ge and Si about which little is known (Wheat and McManus, 2005). The latter hypothesis refers to the possibility of an authigenic enrichment of Ge in reducing sediments, as evoked here above. This hypothesis will be tested in the following sections.

5.2. Authigenic enrichment in reducing sediments

In this section we shall observe ancient sediments that accumulated under more or less drastically limited conditions of bottom oxygenation, and variable conditions of surface productivity. In other words, most of the sediments were bathed by reducing pore waters and we want to try to detect possible Ge enrichment. In addition, if Ge enrichment is detected, is it decoupled from the Si content?

5.2.1. La Serre Section — Frasnian–Famennian boundary

The good positive correlation between Al_2O_3 and SiO_2 indicates rather constant proportions for the components of the aluminosilicate fraction of the sediment. No significant addition of quartz and/or opal is observed. With Al contents comprised between 0.30 and 6.51% (mean 1.41%), the detrital fraction of the Ge- and U-content of the La Serre samples is expected to fall within the following ranges: for Ge 0.03–0.69 ppm, mean 0.15 ppm; for U 0.06–1.20 ppm, mean 0.26 ppm. It indicates that the two samples belonging to the Upper Kellwasser Horizon show a significant (authigenic) enrichment in both Ge (0.4 ppm and 0.8 ppm) and U (ca. 12 ppm). In other words, the two samples that underwent reducing conditions (U enrichment) show a slight but significant enrichment in Ge. This enrichment is also visible in Fig. 1B where these two samples plot above the regression line corresponding to the Ge/ SiO_2 ratio of the upper crust (data from McLennan, 2001), that represents the clastic supply.

5.2.2. The Jurassic of the Boulonnais

For the Argiles de Wimereux and Argiles de Châtillon formations, most samples indicate that Ge is carried by the aluminosilicate fraction of the sediment. In each of the two formations, two samples record a relative depletion in Ge compared to SiO_2. It suggests that these samples contain a more abundant fraction of quartz or biogenic opal. The important point is that, concerning the Bancs Jumeaux Formation, the samples with a significant enrichment factor in Mo (i.e., N10, cf. Algeo and Tribovillard, 2009) are those with the highest

enrichment factor in Ge. The only sample with a significant (N10) U-EF (U-EF~100) is the most enriched in Ge. This simultaneous enrichment in Ge and in redox-sensitive elements (U and Mo) is not observed for the rest of the Bancs Jumeaux samples or for the samples of the Argiles de Wimereux and Argiles de Châtillon formations, where no significant enrichment in redox proxies is observed. For all these samples that did not record reducing depositional conditions, the dominant Ge carrier-phase is the aluminosilicate fraction of the sediment.

Largely, the samples of the Argiles de Wimereux and Bancs Jumeaux formations fall on or close to the clastic Ge/ SiO_2 regression line (Fig. 2B and H), which confirms that most of the sediments are not enriched or depleted in Ge relative to crustal values. The samples of the Argiles de Châtillon Formation plot above the clastic line (Fig. 2E), but this situation results from the fact that the samples of this formation are somewhat depleted in SiO_2 relative to the Al_2O_3 content (Fig. 2D).

5.2.3. The Weddell Sea site — Early Cretaceous

As for the La Serre Section, the good positive correlation between Al_2O_3 and SiO_2 (close to crustal proportions; Fig. 3A) indicates rather constant proportions in the components of the aluminosilicate fraction. Again, no significant addition of quartz and/or opal is observed. Germanium is poorly correlated to SiO_2 (the same is true if Al_2O_3 is considered instead of SiO_2), which suggests that the aluminosilicate fraction is not the only supplier of Ge. If Si correlates with Al (terrigenous supply) but Ge does not correlate with Si, then it is inferred that part of the Ge content is of authigenic origin. The authigenic enrichment is also evidenced by the samples plotting above the clastic Ge- SiO_2 regression line (Fig. 3B). The fact that the samples with the highest Ge-EF are the ones with the highest U-EF suggests again that the most Ge-enriched samples were deposited under reducing conditions (U enrichment).

5.2.4. The Bahloul Formation (Upper Cretaceous)

Again, as for the previous cases, it is observed that the samples that underwent reducing depositional conditions reflected by detectable or significant Mo enrichments are also those yielding the most pronounced enrichment in Ge. Most samples plot above the clastic Ge- SiO_2 regression line (Fig. 4B), which would indicate some authigenic Ge enrichment but the SiO_2– Al_2O_3 content of the Bahloul Formation does not match exactly that of the average upper crust (Fig. 4A).

5.2.5. Discussion

We observe in the previous sections that a Ge vs. SiO_2 crossplot may give a good estimate of the main source of Ge, comparing the sample location relative to the Ge– SiO_2 regression line of the average crust composition. Points falling on or close to the regression line will testify to a clastic Ge supply; points falling above the regression line should indicate an authigenic enrichment in Ge, decoupled from silica diagenesis; points situated below the line would indicate the presence of Ge-poor biogenic silica (lowered Ge/ SiO_2). These statements only hold if the studied formations have a SiO_2– Al_2O_3 composition close to that of average crust, which is of course not always the case (cf. the Argiles de Châtillon Formation). To level this difficulty, a more detailed approach is conducted using enrichment factors. For this purpose, observing the SiO_2 vs. Al_2O_3 distribution is of cornerstone importance. We calculate enrichment factors where the concentration of Ge is compared to that of Al. If a biogenic opal fraction is added to the sediments, it will bring some Ge but no Al, hence an increase in the Ge-EF. However this increase of the Ge-EF will not correspond to any authigenic enrichment but it will simply echo the biogenic opal supply. The same reasoning also holds if quartz is considered instead of biogenic opal, because quartz will also bring Ge but no Al. In the case of the Jurassic

formations of the Boulonnais, SiO_2 and Al_2O_3 are rather poorly correlated, which must be ascribed to variable quartz supply in a proximal ramp setting. However, the samples of the Bancs Jumeaux Formation with the highest Ge-EF do not have the highest SiO_2 content, which indicates that the high Ge-EF is not induced by a high quartz content but rather by an authigenic Ge incorporation. In the case of the La Serre Section, Weddell Sea and Bahloul Formation, SiO_2 and Al_2O_3 draw clear correlations, which rules out any significant variation in the supply of opal or quartz. Consequently, under such conditions, increases in the Ge-EF can be ascribed to authigenic enrichment of Ge and may be decoupled from the SiO_2 content. This decoupling is well illustrated by the La Serre and Weddell Sea samples showing a marked enrichment in redox proxies U and Mo. In these cases, the samples underwent strongly reducing conditions that favored the authigenic capture of Ge as indicated by the poor covariation of Ge and SiO_2, whereas the Bahloul Formation endured less drastic redox conditions as illustrated by only few samples with Mo- and U-EF exceeding the value 5.

In this paper, we deal with germanium that is naturally occurring with very low abundance in sedimentary particles, either terrigenous or hydrogenous. Although the sources and sinks for methyl Ge in the ocean are still poorly known, interconversion of the organic and inorganic Ge species may be ruled out, to the best of our knowledge. In addition, Ge(IV) does not undergo reduction to Ge(II) under Earth surface conditions (King et al., 2000). As Ge is not redox-sensitive, it cannot have high enrichment factor values, in sharp contrast to redox proxies such as U and Mo, capable to reach very high enrichment factors (tens to hundreds or even more; Tribovillard et al., 2004c) owing to a redox-triggered change in their chemical status and behavior. In the sedimentary environments discussed here, the parameters of Ge always remain in a narrow range of values: maximal concentrations encountered in this study do not exceed 3 ppm and enrichment factor values keep low, commonly b5,

occasionally bracketed between 5 and 9 for some Bahloul samples, and reaching exceptionally 15 in the early Cretaceous of the Weddell Sea site. However, our results show that samples deposited under reducing conditions evidenced by detectable or strong enrichments in U and/or Mo all yield enrichments en Ge. The enrichments are always weak, as said above, but they are systematic, which strongly suggests that the enrichments are significant.

This in-depth discussion about authigenic Ge enrichment of sediments deposited under more or less severely reducing conditions may be summarized using crossplots opposing the enrichment-factor values of redox proxies such as U and Mo to the values of the Ge/Si ratio of sediments (Fig. 6). Formations deposited under dominantly reducing conditions show a positive correlation between the enrichment factors of Mo (e.g., the Bahloul Formation; Fig. 6B) or U (e.g., the Weddell Sea; Fig. 6C) and the Ge/Si ratio, whereas formations deposited under oxic to occasionally suboxic conditions do not show such positive correlation (e.g., the Jurassic formations of the Boulonnais; Fig. 6A).

Lastly, with our available data, we cannot identify any authigenic mineral that could have captured Ge from seawater and trapped it durably.

6. Conclusion

Our preliminary results suggest that radiolarians can transfer germanium from seawater to sediments in proportions similar to, or possibly slightly above, those observed for diatoms. However the results are still limited and must be considered with caution. Our study, basing on sedimentary data spanning a large time interval shows that sediments deposited under reducing conditions may capture Ge from seawater. We can thus confirm the interpretation of an authigenic enrichment of Ge in recent, reducing sediments formulated by Hammond et al. (2000), King et al. (2000) and McManus et al. (2003) basing on analyses of pore water, benthic incubations and core incubations from study sites located on the California and Peru/Chile margins. We observed here Ge

capture in various past environments where depositional conditions were reducing. This observation is of importance to complement our understanding of the Ge cycle that is not completely constrained yet. Reducing sediments partly uncouple Ge from Si burial, which allows sequestering Ge in marine sediments in proportions that are higher that what can be expected from biogenic opal alone. Hence, during geological episodes prone to the development of anoxia in bottom waters, reducing sediments located in platform or deep settings or below upwelling systems will subtract Ge from the seawater inventory. Depending on the scale of the phenomenon (extent and duration) it may lower the seawater Ge/Si ratio but may not mean that the flux of Ge released to the ocean through continental/ submarine weathering or hydrothermalism had changed. Now the challenge is to identify the actual authigenic phase capable to capture Ge and sequester it durably at the geological timescale.

Acknowledgements

We thanks François Guillot for fruitful discussions about germanium, Olivier Averbuch for supplying samples of the Argiles de Wimereux Formation, and Annachiara Bartolini and Sylvia Gardin for kindly sharing their geochemical data of ODP site 692. Thanks to the two anonymous referees who helped us improve significantly the manuscript and to Joel D. Blum for the editorial work as well as Jules Snelleman of the editorial office of Chemical Geology.

Appendix A. Supplementary data

Supplementary data to this article can be found online at doi:10.1016/j.chemgeo.2011.01.015.

References

Algeo, T.J., Maynard, J.B., 2004. Trace-element behavior and redox facies in

core shales of Upper Pennsylvanian Kansas-type cyclothems. Chemical Geology 206, 289–318.

Algeo, T.J., Tribovillard, N., 2009. Environmental analysis of paleoceanographic systems based on molybdenum-uranium covariation. Chemical Geology 268, 211–225.

Averbuch, O., Tribovillard, N., Devleeschouwer, X., Riquier, L., Mistiaen, B., Van Vliet- Lanoe, B., 2005. Mountain building-enhanced continental weathering and organic carbon burial as major causes for climatic cooling at the Frasnian–Famennian boundary (ca 376 Ma BP). Terra Nova 17, 33–42.

Azam, F., 1974. Silicic acid uptake in diatoms studies with 68Ge germanic acid as tracer. Planta 121, 205–212.

Azam, F., Chisholm, S.W., 1976. Silicic acid uptake and incorporation by natural marine phytoplankton populations. Limnology and Oceanography 21, 427–435.

Azam, F., Hemmingsen, B.B., Volcani, B.E., 1973. Germanium incorporation into the silica of diatom cell walls. Arch. Microbiol. 92, 11–20 doi:10.1007/BF00409507.

Bareille, G., Labracherie, M., Mortlock, R.A., Maier-Reimer, E., Froelich, P.N., 1998. A test of (Ge/Si)opal as a paleorecorder of (Ge/Si)seawater. Geology 26 (2), 179–182.

Barker, P.E., Kennett, J.P., et al., 1988. Proc. ODP, Init. Repts. Ocean Drilling Program, College Station, TX, p. 113 doi:10.2973/odp.proc.ir.113.1988.

Bernstein, L.R., 1985. Germanium geochemistry and mineralogy. Geochim. Cosmochim. Acta 49, 409–2422.

Bruland, K.W., Lohan, M.C., 2003. Controls of trace metals in seawater. In: Elderfield, H. (Ed.), The Ocean and Marine Geochemistry. : In: Holland, H.D., Turekian, K.K. (Eds.), Treatise on Geochemistry, 6. Elsevier-Pergamon, Oxford, pp. 23–47.

Brumsack, H.-J., 2006. The trace metal content of recent organic carbon-rich

sediments: implications for Cretaceous black shale formation. Palaeogeography, Palaeoclimatology, Palaeoecology 232, 344–361.

Canfield, D.E., Thamdrup, B., 2009. Towards a consistent classification scheme for geochemical environments, or, why we wish the term ‘suboxic’ would go away. Geobiology 7, 385–392.

Carignan, J., Hild, P., Morel, J., Yeghicheyan, D., 2001. Routine analysis of trace elements in geochemical samples using flow injection and low-pressure on-line liquid chromatography coupled to ICP-MS: a study of geochemical references materials BR, DR-N, UB-N, AN-G and GH. Geostandard Newsletter 25, 187–198.

Caron, M., Robaszynski, F., Amédro, F., Baudin, F., Deconinck, J.-F., Hochuli, P., Von Salis- Perch-Nielsen, K., Tribovillard, N., 1999. Duration of the oceanic anoxic event at the Cenomanian Turonian boundary. Cyclostratigraphic interpretation of the Bahloul Formation in Central Tunisia. Bulletin de la Société Géologique de. France 170 (2),145–160.

Chester, R., 2000. Marine Geochemistry, Second Edition. Blackwell Science Ltd. 506 pp.

Deconinck, J.-F., Geyssant, J.R., Proust, J.-N., Vidier, J.P., 1996. Sédimentologie et biostratigraphie des dépôts kimméridgiens et tithoniens du Boulonnais. Annales de la Société Géologique du Nord 4, 157–170.

Ellwood, M.J., Maher, W.A., 2003. Germanium cycling in the waters across a frontal zone: the Chatam Rise, New Zealand. Mar. Chem. 80, 145–159.

Ellwood, M.J., Kelly, M., Maher, W.A., De Deckker, P., 2006. Germanium incorporation into sponge spicules: development of a proxy for reconstructing inorganic germanium and silicon concentrations in seawater. Earth Planet. Sci. Lett. 243, 749–759

Feist, R., 1985. Devonian stratigraphy of the South-eastern Montagne Noire (France). Cour. Forsch Inst. Senckenberg 75, 331–352.

Froelich, P.N., Andreae, M.O., 1981. The marine geochemistry of germanium

— ekasilicon. Science 13, 205–207.

Froelich, P.N., Hambrick, G.A., Andreae, M.O., Mortlock, R.A., Edmond, J.M., 1985a. The geochemistry of inorganic germanium in natural waters. Journal of Geophysical Research — Oceans 90, 1133–1141.

Froelich, P.N., Kaul, L.W., Bird, J.T., Andreae, M.O., Roe, K.K., 1985b. Arsenic, barium, germanium, tin, dimethylsulfide and nutrient biogeochemistry in Charlotte Harbor, Florida, a phosphorus-enriched estuary. Estuar. Coastal Shelf Sci. 20, 239–264.

Froelich, P.N., Mortlock, R.A., Shemesh, A., 1989. Inorganic germanium and silica in the Indian ocean: biological fractionation during (Ge/Si)opal formation. Global Biogeochemical Cycles 3, 79–88.

Froelich, P.N., Vlanc, V.R., Mortlock, R.A., Chilled, S.N., Dustan, W., Udomkit, A., Peng, T.H., 1992. River fluxes of dissolved silica to the ocean were higher during glacials: Ge/Si in diatoms, rivers and oceans. Paleoceanography 7, 739–767.

Hammond, D.E., McManus, J., Berelson, W.M., Meredith, C., Klinkhammer, G.P., Coale, K.H., 2000. Diagenetic fractionation of Ge and Si in reducing sediments: the missing Ge sink and a possible mechanism to cause glacial/interglacial variations in oceanic Ge/Si. Geochimica et Cosmochimica Acta 64, 2453–2465.

Hammond, D.E., McManus, J., Berelson, W.M., 2004. Oceanic germanium: silicon ratios: evaluation of the potential overprint of temperature on weathering signals. Paleooceanography 19, PA2016 doi:10.1029/2003JF000026.

Höll, R., Kling, M., Schroll, E., 2007. Metallogenesis of germanium — a review. Ore Geology Reviews 30, 145–180.

King, S.L., Froelich, P.N., Jahnke, R.A., 2000. Early diagenesis of germanium in sediments of the Antarctic South Atlantic: in search of the missing Ge sink. Geochimica et Cosmochimica Acta 64, 1375–1390.

Kolodny, Y., Halicz, L., 1988. The geochemistry of germanium in deep-sea

cherts. Geochimica et Cosmochimica Acta 52, 2333–2336.

McLennan, S.M., 2001. Relationships between the trace element composition of sedimentary rocks and upper continental crust. Geochemistry, Geophysics, Geosystems (G3) 2 paper # 2000GC000109..

McManus, J., Hammond, D.E., Cummins, K., Klinkhammer, G.P., Berelson, W.M., 2003. Diagenetic Ge#Si fractionation in continental margin environments: further evidence for a nonopal Ge sink. Geochim. Cosmochim. Acta 67 (23), 4545–4557.

Mortlock, R.A., Froelich, P.N., 1987. Continental weathering of germanium — Ge/Si in the global river discharge. Geochimica et Cosmochimica Acta 51, 2075–2082.

Mortlock, R.A., Froelich, P.N., Feely, R.A., Massoth, G.J., Butterfield, D.A., Lupton, J.E., 1993. Silica and germanium in Pacific Ocean hydrothermal vents and plumes. Earth Planet. Sci. Lett. 119, 65–378.

Murnane, R.J., Leslie, B., Hammond, D.E., Stallard, R.F., 1989. Germanium geochemistry in the Southern-California borderlands. Geochimica et Cosmochimica Acta 53, 2873–2882.

Pokrovski, G.S., Schott, J., 1998. Thermodynamic properties of aqueous Ge(IV) hydroxide complexes from 25 to 350 degrees C: implications for the behavior of germanium and the Ge/Si ratio in hydrothermal fluids. Geochimica et Cosmochimica Acta 62, 1631–1642.

Proust, J.-N., Deconinck, J.-F., Geyssant, J.R., Herbin, J.-P., Vidier, J.P., 1995. Sequence analytical approach to the Upper Kimmeridgian-Lower Tithonian storm-dominated ramp deposits of the Boulonnais (Northern France). — a landward time equivalent to offshore marine source rocks. Geol. Rundsch. 84, 255–271.

Randon, C., Nutthawut, W., Caridroit, M., Perret-Mirouse, M.-F., Degardin, J.-M., 2006. Upper Devonian-lower Carboniferous conodonts from Chiang Dao Chert, Northern Thailand. Rivista Italiana di Paleontologia e Stratigrafia 112,

191–206.

Riquier, L., Tribovillard, N., Averbuch, O., Devleeschouwer, X., Riboulleau, A., 2006. The Late Frasnian Kellwasser horizons of the Harz Mountains (Germany): two oxygen deficient periods resulting from different mechanisms. Chemical Geology 233, 137–155.

Riquier, L., Averbuch, O., Tribovillard, N., El Albani, A., Lazreq, N., Chakiri, S., 2007. Environmental changes at the Frasnian–Famennian boundary in Central Morocco (Northern Gondwana): integrated rock-magnetic and geochemical studies. In:

Becker, T., Kirchgasser, B. (Eds.), Devonian Events and Correlations. : Special Publications, 278. Geological Society, London, pp. 197–217.

Savrda, C.E., Bottjer, D.J., 1991. Oxygen-related biofacies in marine strata: an overview and update. In: Tyson, R.V., Pearson, T.H. (Eds.), Modern and Ancient Continental Shelf Anoxia: Geol. Soc. London Spec. Publ., 58, pp. 201–219.

Shemesh, A., Mortlock, R.A., Smith, R.J., Froelich, P.N., 1988. Determination of Ge/Si in marine siliceous microfossils: separation, cleaning and dissolution of diatoms and radiolaria. Marine Chemistry 25, 305–323.

Shemesh, A., Mortlock, R.A., Froelich, P.N., 1989. Late Cenozoic Ge/Si record of marine biogenic opal: implications for variations of riverine fluxes to the ocean. Paleoceanography 3, 221–234.

Sutton, J., Ellwood, M.J., Maher, W.A., Croot, P.L., 2010. Oceanic distribution of inorganic germanium relative to silicon: germanium discrimination by diatoms. Global Biogeochemical Cycles 24, GB2017 doi:10.1029/2009GB003689.

Taylor, S.R., McLennan, S.M., 1985. The continental crust: its composition and evolution. Blackwell, Oxford. 312 pp.

Tolmacheva, T.J., Danelian, T., Popov, L.E., 2001. Evidence for 15 m.y. of continuous deep-sea biogenic siliceous sedimentation in early Paleozoic oceans.

Geology 29, 755–758.
Tribovillard, N., Bialkowski, A., Tyson, R.V., Vergès, E., Deconinck, J.-F., 2001. Organic facies and sea level variation in the Late Kimmeridgian of the Boulonnais area (northernmost France). Marine and Petroleum Geology 18, 371–389.
Tribovillard, N., Averbuch, O., Bialkowski, A., Deconinck, J.-F., 2002. The influence of the early diagenesis of marine organic matter on the magnetic-susceptibility signal of sedimentary rock. Bulletin de la Société Géologique de France 173, 295–306.
Tribovillard, N., Averbuch, O., Devleeschouwer, X., Racki, G., Riboulleau, A., 2004a. Deep-water anoxia over the Frasnian–Famennian boundary (La Serre, France): a
tectonically-induced oceanic anoxic event? Terra Nova 16 (5), 288–295.
Tribovillard, N., Trentesaux, A., Ramdani, A., Baudin, F., Riboulleau, A., 2004b. Contrôles de l'accumulation de matière organique dans la Kimmeridge Clay Formation (Jurassique supérieur, Yorkshire, G.B.) et son équivalent latéral du Boulonnais: l'apport des éléments traces métalliques. Bulletin de la Société Géologique de France 175 (5), 491–506.
Tribovillard, N., Riboulleau, A., Lyons, T., Baudin, F., 2004c. Enhanced trapping of molybdenum by sulfurized organic matter of marine origin as recorded by various Mesozoic formations. Chemical Geology 213, 385–401.
Tribovillard, N., Algeo, T., Lyons, T.W., Riboulleau, A., 2006. Trace metals as paleoredox and paleoproductivity proxies: an update. Chemical Geololy 232, 12–32.
Tribovillard, N., Lyons, T.W., Riboulleau, A., Bout-Roumazeilles, V., 2008. A possible capture of molybdenum during early diagenesis of dysoxic sediments. Bulletin de la Société Géologique de France 179, 3–12.
Tyson, R.V., 1995. Sedimentary Organic Matter: Organic Facies and Palynofacies. Chapman & Hall, London. 615 pp.

Van der Weijden, C.H., 2002. Pitfalls of normalization of marine geochemical data using a common divisor. Marine Geology 184, 167–187.
Wedepohl, K.H., 1971. Environmental influences on the chemical composition of shales and clays. In: Ahrens, L.H., Press, F., Runcorn, S.K., Urey, H.C. (Eds.), Physics and chemistry of the Earth. Oxford, Pergamon, pp. 305–333.
Wedepohl, K.H., 1991. The composition of the upper Earth's crust and the natural cycles of selected metals. In: Merian, E. (Ed.), Metals and their compounds in the Environment. VCH-Verlagsgesellschaft, Weinheim, pp. 3–17.
Wheat, C.G., McManus, J., 2005. The potential role of ridge-flank hydrothermal systems on oceanic germanium and silicon balances. Geochimica et Cosmochimica Acta 69, 2021–2029.
Wignall, P.B., 1994. Black Shales. Clarendon Press, Oxford. 127 pp. 130 N. Tribovillard et al. / Chemical Geology 282 (2011) 120–130

Figure captions

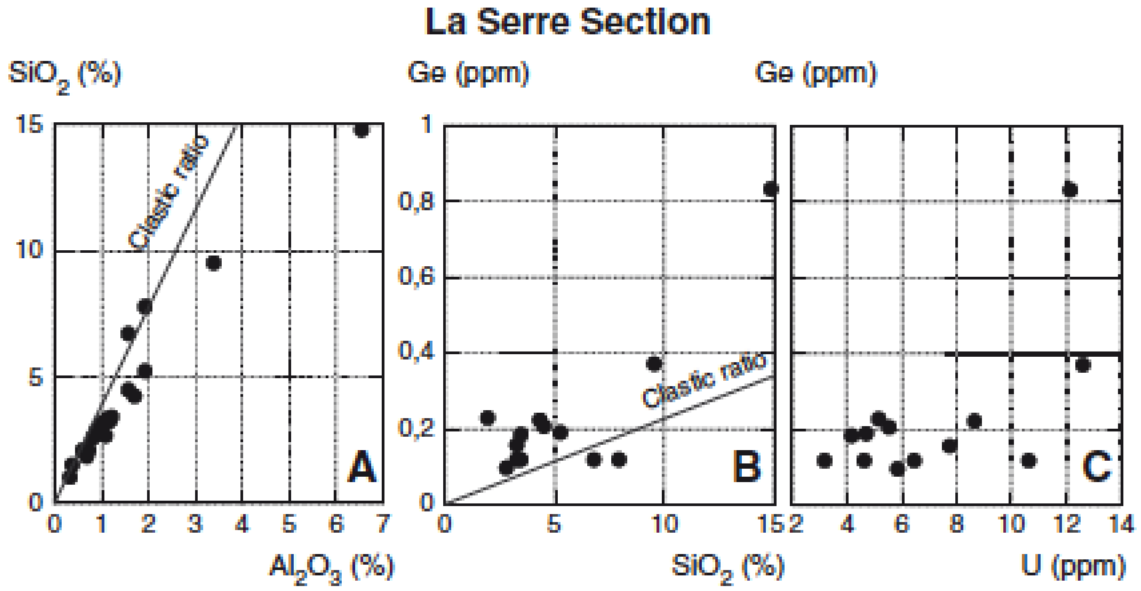

Fig. 1. Characteristic chemical concentrations of the 13 samples of the La Serre Section, late Devonian, Southern France, illustrated by 3 crossplots: SiO_2 vs. Al_2O_3 (A); Ge vs. SiO_2 (B); Ge vs. U (C).

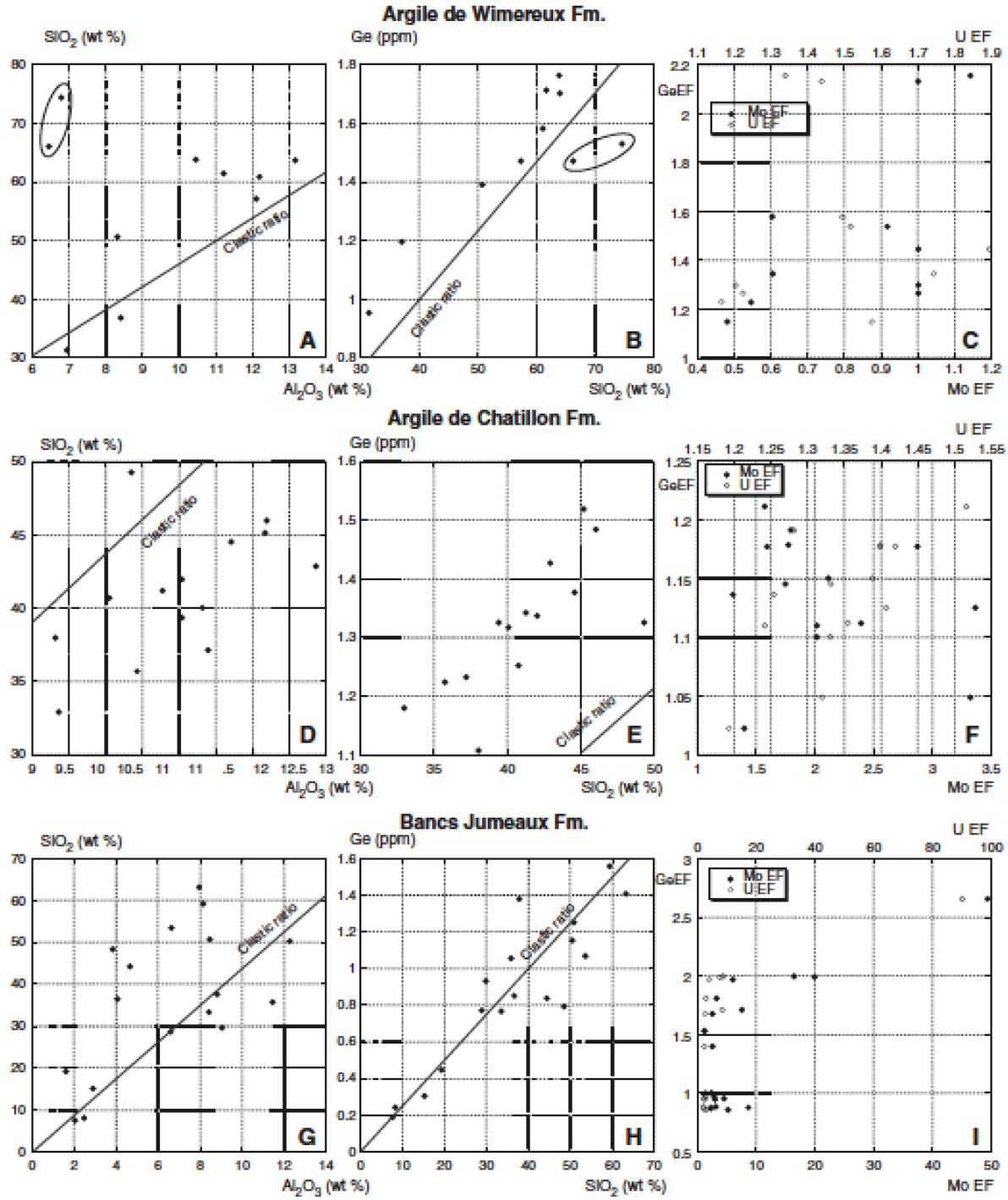

Fig. 2. Characteristic data of the studied three formations of the Boulonnais area (late Jurassic, Northernmost France). A to C: Argiles de Wimereux; D to F: Argiles de Châtillon; G to I: Bancs Jumeaux. EF stands for enrichment factors; see definition and explanations in text

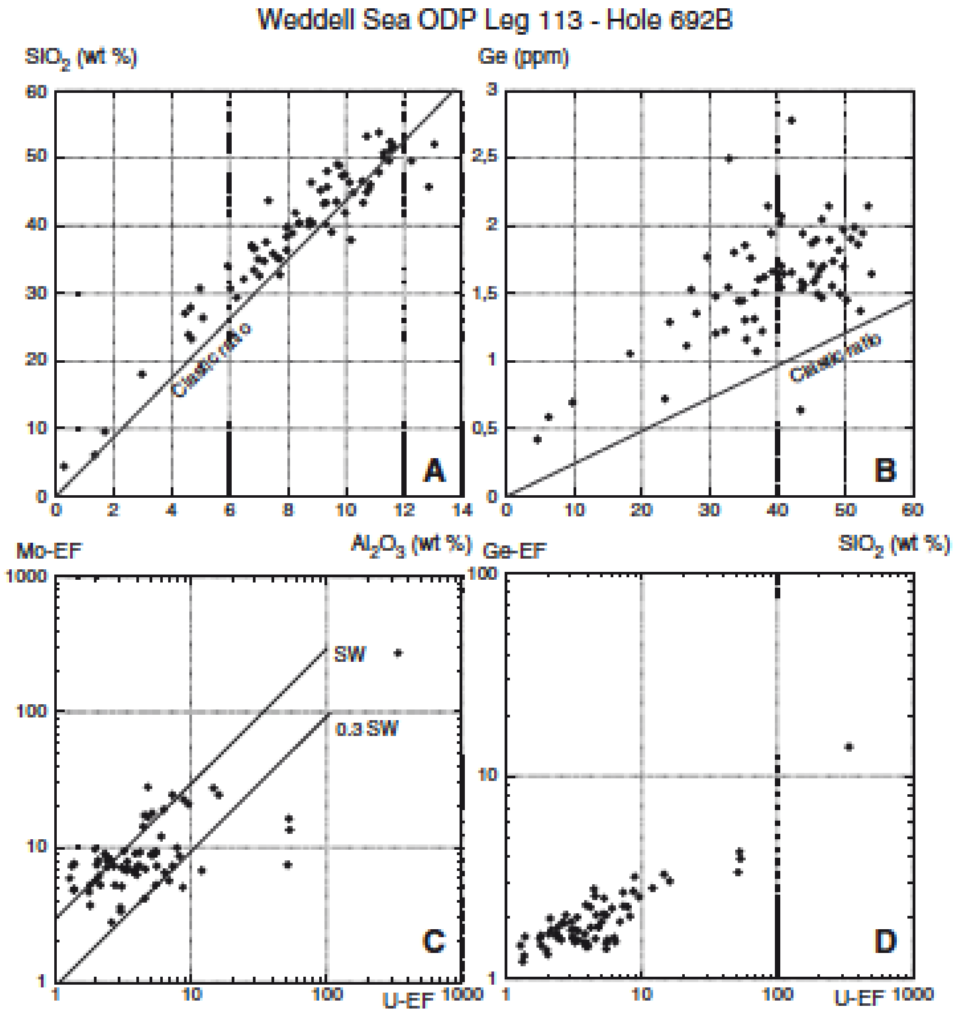

Fig. 3. Characteristic data of the Cretaceous section of ODP site 692B (Leg 113, Weddell Sea) showing the relationships between SiO_2 and Al_2O_3 (A) and Ge and SiO_2 (B). C: location of the samples in a crossplot opposing U- to Mo-enrichment factor (EF) values as defined by Algeo and Tribovillard (2009). The diagonal lines show the Mo/U molar ratio equal to the seawater value (SW) and to a fraction thereof (0.3°—SW). D: Relationship between the enrichment factor (EF) values of U, Mo and Ge.

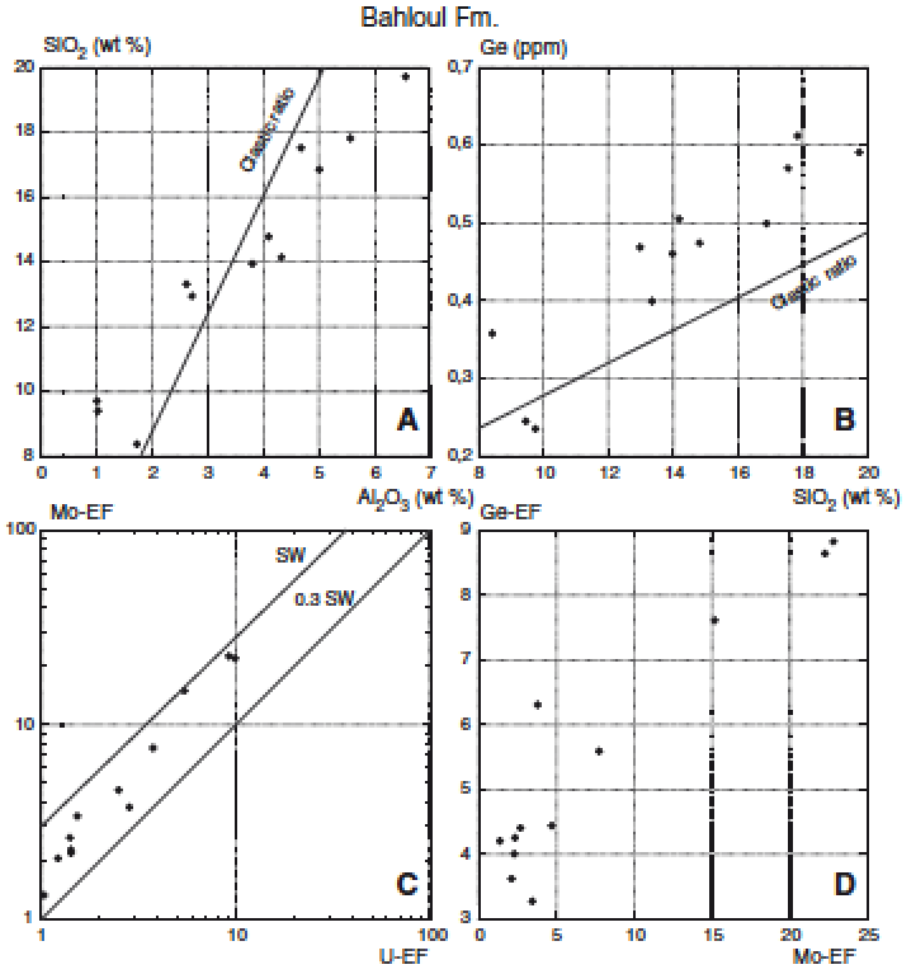

Fig. 4. Characteristic data of the samples of the Cretaceous Bahloul Formation in the Wadi Bahloul section, Central Tunisia, showing the relationships between SiO_2 and Al_2O_3 (A) and Ge and SiO_2 (B). C: location of the samples in a crossplot opposing U- to Mo-enrichment factor (EF) values as defined by Algeo and Tribovillard (2009). The diagonal lines show the Mo/U molar ratio equal to the seawater value (SW) and to a fraction thereof (0.3°—SW). D: Relationship between the enrichment factor (EF) values of U, Mo and Ge.

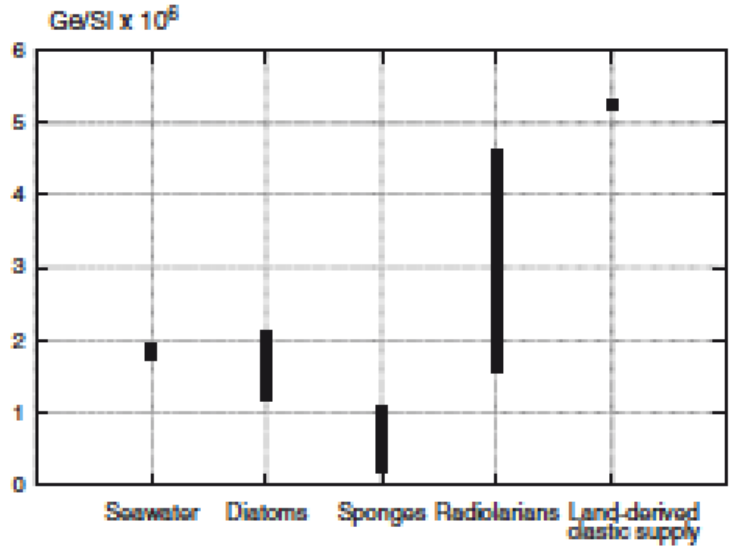

Fig. 5. Values of the Ge/Si ratio of the mean terrigenous supply, seawater and main opalsecreting organisms.

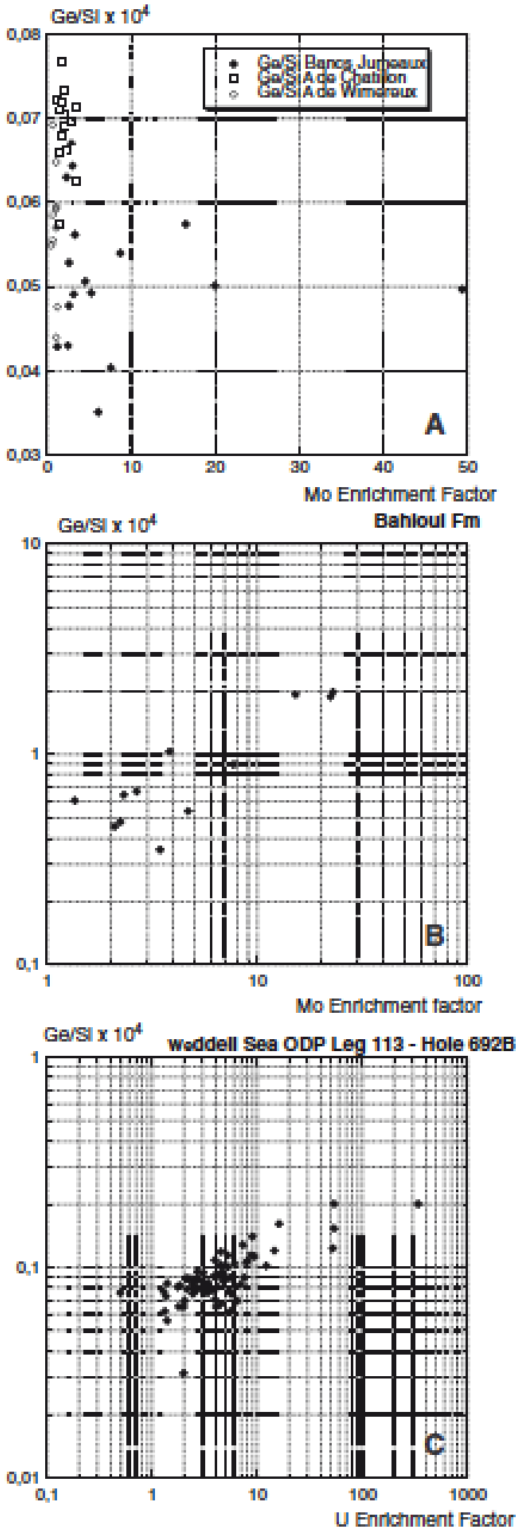

Fig. 6. Crossplots opposing the values of the enrichment factors of Mo (A and B) or U (C) to those of the Ge/Si ratio.

Table 1

Comparison of silicon and germanium regarding their sources and sinks, as well as residence time in the ocean.

	Silicon	Germanium	References
Dominant supply to modern ocean	River supply (5.6×10^{12} mol y^{-1}) with minor contributions from aeolian sources, hydrothermal input, and low-temperature basalt weathering (these minor sources amounting 1.4×10^{12} mol y^{-1})	Two primary sources: rivers (3.3×10^{6} mol y^{-1}) and hydrothermal inputs (4.9 to 7.1×10^{6} mol y^{-1}); aeolian inputs and low-temperature basalt weathering each contributing 0 to 0.4×10^{6} mol y^{-1}	Mortlock et al., 1993; King et al., 2000; Wheat and McManus, 2005
Residence time in the oceans	<20 kyr	<10 kyr	Hammond et al. (2004)
Main sink	Marine biogenic sediments (primarily as diatoms, sponges, and radiolaria + silicoflagellates) totaling $6.5–7.4 \times 10^{12}$ mol y^{-1}	Biogenic opal, accounting for 4.8×10^{6} mol y^{-1}, i.e., nearly half of the Ge oceanic input with the balance (5.4×10^{6} mol y^{-1}) being burial within a non-opaline phase that forms in iron-rich reducing sedimentary environments	Hammond et al., 2000; King et al., 2000; McManus et al., 2003; Wheat and McManus, 2005

Table 2

Detection thresholds and accuracy for the analyses presented in this work.

Elements	Detection threshold	Accuracy (%)
SiO_2	0.05%	<1
Al_2O_3	0.02%	<1
Fe_2O_3	0.04%	<2
Ge	0.05 ppm	<5
Mo	0.40 ppm	<5
U	0.05 ppm	<8

Table 3

Geochemical data of the radiolarite samples studied here

Formations	Sample #	SiO_2 wt. %	Al_2O_3 wt. %	Ge ppm	Ge/Si× 10^{-6}	Ge_{terr} ppm	Ge_{bio} ppm	Si_{terr} wt%	Si_{bio} wt%	$(Ge/Si)_{bio}\times10^{-6}$
Burubaital	89101/C1	95.95	2.28	0.63	1.40	0.24	0.39	4.61	40.24	0.97
	89101/F33a	97.72	0.65	0.32	0.70	0.07	0.25	1.32	44.36	0.56
	89101/F33b	99.10	0.34	0.67	1.46	0.04	0.64	0.69	45.63	1.40
	89101/37.2	96.24	1.35	1.00	2.23	0.14	0.86	2.74	42.25	2.03
	89101/12.3	97.35	0.51	1.00	2.20	0.05	0.95	1.04	44.47	2.13
	89101/C5	97.40	1.21	0.75	1.65	0.13	0.63	2.46	43.07	1.45
	89101/F18	97.61	0.77	0.74	1.63	0.08	0.66	1.56	44.07	1.50
	89101/35.0	96.50	1.17	0.37	0.83	0.12	0.25	2.37	42.74	0.59
	89101/E30a	95.94	0.60	0.71	1.58	0.06	0.65	1.22	43.63	1.48
	89101/E30b	98.33	0.12	1.06	2.31	0.01	1.05	0.23	45.73	2.30
	89101/E30c	97.91	0.14	1.76	3.85	0.01	1.75	0.28	45.49	3.85
	9706/16.00	95.02	0.95	0.64	1.45	0.10	0.54	1.93	42.48	1.28
	9706/34.4	96.70	0.83	0.62	1.37	0.09	0.53	1.67	43.52	1.22
	Mean	97.06	0.84	0.79	1.74	0.09	0.70	1.70	43.67	1.61
Chiang Dao Chert	B 24	89.20	3.95	1.90	4.56	0.41	1.49	8.00	33.69	4.42
	B 30	98.29	0.62	1.51	3.30	0.07	1.45	1.26	44.68	3.24
	B 35	89.83	4.72	2.16	5.15	0.50	1.67	9.57	32.42	5.14
	B 41	92.68	0.78	1.48	3.40	0.08	1.39	1.59	41.74	3.34
	B 46	85.56	7.72	3.10	7.74	0.81	2.28	15.65	24.34	9.39
	B 62	90.09	2.65	1.91	4.55	0.28	1.64	5.38	36.73	4.45
	Mean	91.76	3.04	1.81	4.22	0.32	1.49	6.16	36.73	4.06